Applied Mathematics and Mechanics
(English Edition, Vol. 13, No. 5, May 1992)

Published by SUT,
Shanghai, China

ON THE APPLICATION OF ADI METHOD TO NUMERICAL SIMULATION OF THE MARANGONI CONVECTION CONTROLLING IN LIQUID BRIDGE MODEL*

Huang Wei-zhang (黄维章) Zhang Suo-chun (张锁春) Xie Zuo-heng (谢佐恒)

(Institute of Applied Mathematics, Academia Sinica, Beijing)

Li Jia-chun (李家春)

(Institute of Mechanics, Academia Sinica, Beijing)

(Received May 11, 1991)

Abstract

An ADI scheme is suggested to simulate the Marangoni convection controlling with emphasis on investigating application of the technique numerically. Numerical experiments conducted in the present paper turn out both successful and efficient. Hence, ADI scheme is expected to be extended to the study of other convection processes related to material manufacturing.

Key words Marangoni convection, liquid bridge, ADI

I. Introduction

It is a common impression that usually natural convection driven by bouyancy will no longer occur in low- or micro-gravity environments. This kind of phenomenon may provide an ideal condition for manufacturing high quality materials. Nevertheless, in the liquid bridge model of crystal growth experiment in a floating zone, the complicated flow due to surface tension will become dominant over those due to other factors. It is of significance for us to gain a penetrating insight into this complicated flow through numerical simulation so as to avoid unnecessary failure in the experiments aboard spacecraft.

In this paper we concentrate on the numerical simulation of the Marangoni convection controlling in the liquid bridge model by using one of the finite difference schemes: implicit alternating directions iterative method (ADI method). Numerical experiments conducted in the present paper show that the ADI method is both successful and efficient in the computation, especially for medium Reynolds number cases.

II. Mathematical Formulation

Consider the liquid bridge model of crystal growth experiment in a floating zone, in which the Marangoni convection due to surface tension becomes prevailing. The configuration studied is illustrated in Fig. 1.

---

* The project supported by the National Natural Science Foundation of China

A liquid bridge is formed between two differentially heated cylindrical rods. The top one is maintained at a higher constant temperature while the bottom one at a lower constant temperature. The surface tension gradient induced by the heterogeneous temperature distribution on the free surface of the liquid bridge is the main factor to drive melt in motion.

It is assumed as in [2] that the free liquid surface is flat, the flow is incompressible and axisymmetrical, and the heat loss from the free surface to the ambient air is negligible. Under these assumptions the non-dimensionalized differential equations governing the liquid bridge model in cylindrical coordinates (see Fig. 1) are represented in the form of stream function-vorticity as follows

$$\frac{\partial}{\partial t}\zeta=-u\frac{\partial}{\partial r}\zeta-v\frac{\partial}{\partial z}\zeta+\frac{u\zeta}{r}-\frac{Gr}{R_\sigma^2}\frac{\partial\theta}{\partial r}+\frac{1}{R_\sigma}\left[\frac{\partial^2}{\partial r^2}\zeta+\frac{1}{r}\frac{\partial}{\partial r}\zeta-\frac{\zeta}{r^2}+\frac{\partial^2}{\partial z^2}\zeta\right] \tag{2.1a}$$

$$\frac{\partial\theta}{\partial t}=-u\frac{\partial\theta}{\partial r}-v\frac{\partial\theta}{\partial z}+\frac{1}{M_a}\left[\frac{\partial^2\theta}{\partial r^2}+\frac{1}{r}\frac{\partial\theta}{\partial r}+\frac{\partial^2\theta}{\partial z^2}\right] \tag{2.1b}$$

$$0=\frac{\partial^2\psi}{\partial r^2}-\frac{1}{r}\frac{\partial\psi}{\partial r}+\frac{\partial^2\psi}{\partial z^2}-r\zeta \tag{2.1c}$$

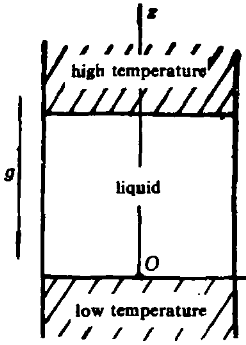

Fig. 1 Simulated floating zone configuration

where r, u and z, v are the radial non-dimensional coordinate, velocity and axial non-dimensional ones respectively, θ is the non-dimensional temperature, parameter $G_r=\beta g\Delta TL^3/\nu^2$ denotes the Grashof number, $R_\sigma=(\partial\sigma/\partial T)\Delta T\cdot(L/\mu\nu)$ —the Reynolds number, $M_a=(\partial\sigma/\partial T)\Delta T\cdot(L/\mu\kappa)$ —the Marangoni number, σ the surface tension, T—the temperature, L—the length, μ and ν the viscous coefficients, β the volume expansion coefficient, κ the heat diffusion coefficient, g the acceleration of gravity. The stream function ψ and vorticity ζ are defined by

$$u=\frac{1}{r}\frac{\partial\psi}{\partial z},\qquad v=-\frac{1}{r}\frac{\partial\psi}{\partial r} \tag{2.2}$$

and

$$\zeta=\frac{\partial u}{\partial z}-\frac{\partial v}{\partial r} \tag{2.3}$$

The boundary conditions are specified as

$$\psi=0,\ \frac{\partial\psi}{\partial z}=0,\ \theta=0 \qquad \text{on } z=0 \tag{2.4a}$$

$$\psi=0,\ \frac{\partial\psi}{\partial z}=0,\ \theta=1 \qquad \text{on } z=1 \tag{2.4b}$$

$$\psi=0,\ \frac{\partial\psi}{\partial r}=0,\ \frac{\partial\theta}{\partial r}=0 \qquad \text{on } r=0 \tag{2.4c}$$

$$\psi=0,\ \zeta=\frac{\partial\theta}{\partial z}-\tau,\ \frac{\partial\theta}{\partial r}=0 \qquad \text{on } r=1 \tag{2.4d}$$

τ in (2.4d), the controlling parameter, represents the value of forces imposed on the free liquid surface by air jet. Specifically, $\tau=0$ means that there is no force applied on the liquid surface.

Equation (2.1) and boundary conditions (2.4) make up the mathematical model describing the controlled Marangoni convection in the liquid bridge model.

III. Difference Schemes

1. General remarks

Scheme 2 in [1], an ADI method, is used for numerical calculation of equation (2.1). The numerical experiments for Taylor vortex in [1] show that this scheme possesses good numerical stability (in particular, for medium Reynolds numbers) and has the advantage of dealing with boundary conditions more easily.

A rectangular mesh is selected for (r, z) domain $[0, 1]\times[0, 1]$.

Let

$$h_r=1/(I-1), \qquad h_z=1/(J-1),$$

where I and J are certain integers, and let

$$\left.\begin{array}{l}\bar{r}_i=(i-1)h_r, \ (i=1,2\cdots,I)\\ \bar{z}_j=(j-1)h_z, \ (j=1,2,\cdots,J)\end{array}\right\} \tag{3.1}$$

Then the mesh is defined by

$$(r_i,z_j)=f(\bar{r}_i),\ f(\bar{z}_j)), \qquad (i=1,\cdots,I;\ j=1,\cdots,J) \tag{3.2}$$

where the function f is defined by

$$f(x)=\frac{\mathrm{th}b\left(x-\frac{1}{2}\right)+\mathrm{th}\frac{b}{2}}{2\mathrm{th}\frac{b}{2}} \tag{3.3}$$

and $b>0$ is an adjusting parameter. The mesh defined in (3.2) is nearly uniform when b is small enough (such as $b=10^{-10}$) by noticing $f(x)\to x$ as $b\to 0$. Thus the uniform mesh is denoted by $b=0$ hereafter for the sake of simplicity.

It is obvious from (3.3) that the bigger b is, the denser the meshes near boundaries are. In contrast, the increment of time Δt is kept invariable in the whole procedure of calculation.

It is assumed that if the values ζ^n , ψ^n and θ^n are given the computational procedure to go ahead from time $n\Delta t$ to time $(n+1)\Delta t$ involves the following steps.

1° Compute ζ^{n+1} from eq. (2.1a), using θ^n,ψ^n and boundary conditions deduced from (2.4).

2° Compute ψ^{n+1} from eq. (2.1b), using ζ^{n+1} and boundary conditions (2.4).

3° Compute θ^{n+1} from eq. (2.1c), using ψ^{n+1},ζ^{n+1} and boundary conditions (2.4).

2. Difference schemes of the equations for vorticity ζ and temperature θ and corresponding boundary conditions

The general form of eqs. (2.1a) and (2.1b) is

$$\frac{\partial\phi}{\partial t}=A\frac{\partial\phi}{\partial z}+B\frac{\partial\phi}{\partial r}+C\phi+D$$

$$+\frac{1}{R}\left[\frac{\partial^2\phi}{\partial r^2}+\frac{1}{r}\frac{\partial\phi}{\partial r}-\beta\frac{\phi}{r^2}+\frac{\partial^2\phi}{\partial z^2}\right] \tag{3.4}$$

where $\beta=1$ for ζ and 0 for θ . Define

$$\Lambda_r=B\frac{\partial}{\partial r}+\frac{1}{R}\left[\frac{\partial^2}{\partial r^2}+\frac{1}{r}\frac{\partial}{\partial r}-\frac{\beta}{r^2}\right]\Big)$$

$$\Lambda_z=A\frac{\partial}{\partial z}+\frac{1}{R}\frac{\partial^2}{\partial z^2} \tag{3.5}$$

and the corresponding difference operators as Λ_{1r}, Λ_{2r} and Λ_{1z}, Λ_{2z},respectively.

Eq. (3.4) is integrated by a method of factorization in two fractional steps:

$$\left.\begin{aligned}&\left(E-\frac{\Delta t}{2}\Lambda_{1z}\right)\phi^*=\left(E+\frac{\Delta t}{2}\Lambda_{2z}\right)\left(E+\frac{\Delta t}{2}\Lambda_{2r}\right)\phi^n\\&\qquad\qquad+\Delta tC\phi^n+\Delta tD\\&\left(E-\frac{\Delta t}{2}\Lambda_{1r}\right)\phi^{n+1}=\phi^*\end{aligned}\right\} \tag{3.6}$$

where E is the identity operator, A, B, C and D take the corresponding values on time $n\Delta t$ the finite difference operators Λ_{1z} and Λ_{2z} are defined by

$$\left.\begin{aligned}\Lambda_{1z}\phi_{i,j}=&\frac{A+|A|}{2}\cdot\frac{\phi_{i,j+1}-\phi_{i,j}}{z_{j+1}-z_j}+\frac{A-|A|}{2}\cdot\frac{\phi_{i,j}-\phi_{i,j-1}}{z_j-z_{j-1}}\\&+\frac{2}{R(z_{j+1}-z_{j-1})}\left[\frac{\phi_{i,j-1}-\phi_{i,j}}{z_{j+1}-z_j}-\frac{\phi_{i,j}-\phi_{i,j-1}}{z_j-z_{j-1}}\right]\\\Lambda_{2z}\phi_{i,j}=&\frac{A+|A|}{2}\cdot\frac{\phi_{i,j}-\phi_{i,j-1}}{z_j-z_{j-1}}+\frac{A-|A|}{2}\cdot\frac{\phi_{i,j+1}-\phi_{i,j}}{z_{j+1}-z_j}\\&+\frac{2}{R(z_{j+1}-z_{j-1})}\left[\frac{\phi_{i,j+1}-\phi_{i,j}}{z_{j+1}-z_j}-\frac{\phi_{i,j}-\phi_{i,j-1}}{z_j-z_{j-1}}\right]\end{aligned}\right\} \tag{3.7}$$

and the finite difference operators Λ_{1r} and Λ_{2r} have similar expressions with Λ_{1z} and Λ_{2z}, respectively.

Eliminating ϕ^* we get for overall step

$$\begin{aligned}\frac{\phi^{n+1}-\phi^n}{\Delta t}=&\frac{1}{2}(\Lambda_{1z}\phi^{n+1}+\Lambda_{2z}\phi^n)+\frac{1}{2}(\Lambda_{1r}\phi^{n+1}+\Lambda_{2r}\phi^n)\\&+C\phi^n+D-\frac{\Delta t}{4}(\Lambda_{1z}\Lambda_{1r}\phi^{n+1}-\Lambda_{2z}\Lambda_{2r}\phi)\end{aligned} \tag{3.8}$$

Scheme (3.8) is consistent with (3.4) with an error for a steady state solution of order $O(h_z^2)+O(h_r^2)+O\left(\Delta t\cdot hz\frac{\partial^2}{\partial z^2}\right)+O\left(\Delta t\cdot h_r\frac{\partial^2}{\partial r^2}\right)$ if a uniform mesh is used. Therefore, we have to restrict time step Δt small enough to minimize the truncation error.

Although scheme (3.6) is not of the second order, we are still capable of yielding solutions with high accuracy by choosing suitable time steps. Notice that in the scheme the operators $\left(E-\frac{\Delta t}{2}\Lambda_{1z}\right)$and $\left(E-\frac{\Delta t}{2}\Lambda_{1r}\right)$ give tridiagonal matrices with diagonal dominance. Then there is no restriction in this scheme on the mesh Reynolds number.

Consider the treatment of corresponding boundary conditions. The boundary conditions for vorticity ζ deduced from eqs. (2.1c) and (2.2)–(2.4) are

$$\left.\begin{aligned}&\zeta=\frac{1}{r}\frac{\partial^2\psi}{\partial z^2}&&\text{on } z=0 \text{ and } z=1\\&\zeta=\frac{1}{2}\frac{\partial^3\psi}{\partial r^3}&&\text{on } r=0\\&\zeta=\frac{\partial\theta}{\partial z}-r&&\text{on } r=1\end{aligned}\right\} \tag{3.9}$$

The treatment of the third equation in (3.9) is trial. The discretization of others in (3.9) is

$$\left.\begin{aligned}
\zeta_{i,1}^{n+1} &= \frac{\alpha}{r_i}\left[\frac{2(z_3-z_1)\psi_{i,2}^n}{(z_2-z_1)^2(z_3-z_2)} - \frac{2(z_2-z_1)\psi_{i,3}^n}{(z_3-z_1)^2(z_3-z_2)}\right] \\
&\quad +(1-\alpha)\zeta_{i,1}^n \qquad\qquad (i=2,\cdots,I-1) \\
\zeta_{i,J}^{n+1} &= \frac{\alpha}{r_i}\left[\frac{2(z_J-z_{J-2})\psi_{i,J-1}^n}{(z_J-z_{J-1})^2(z_{J-1}-z_{J-2})} - \frac{2(z_J-z_{J-1})\psi_{i,J-2}^n}{(z_J-z_{J-2})^2(z_{J-1}-z_{J-2})}\right] \\
&\quad +(1-\alpha)\zeta_{i,J}^n \qquad\qquad (i=2\cdots,I-1) \\
\zeta_{1,j}^{n+1} &= -\frac{3\alpha}{r_3-r_2}\left[\frac{\psi_{2,j}^n}{(r_2-r_1)^2} - \frac{\psi_{3,j}^n}{(r_3-r_1)^2}\right] \\
&\quad +(1-\alpha)\zeta_{1,j}^n \qquad\qquad (j=1,\cdots,J)
\end{aligned}\right\} \tag{3.10}$$

where $\alpha\in(0,1]$ is (boundary) relaxation parameter. If a uniform mesh is used, the first and second formulae are of order 2.

The discretization of boundary conditions on $z=0$ and $z=1$ for temperature θ in (2.4) is trial. The boundary conditions on $r=0$ and $r=1$ for θ in (2.4) are discretized in an order 2 method (c.f.[5]). For instance, the discretization of the boundary condition on $r=0$ is

$$\theta_{1,j}^{n+1} = \frac{(r_3-r_1)^2\theta_{2,j}^{n+1} - (r_2-r_1)^2\theta_{3,j}^{n+1}}{(r_3-r_1)^2-(r_2-{}_1)^2}, \qquad (j=1,\cdots,J) \tag{3.11}$$

The values of ϕ^* on $z=0$ and $z=1$ are needed in scheme (3.6). These values are obtained from the second fractional step applied on the boundary ($z=0$ or $z=1$)

$$\zeta^*|_{z=0} = \left(E - \frac{\Delta t}{2}\Lambda_{1r}\right)\zeta_{z=0}^{n+1} \tag{3.12}$$

3. Difference scheme of equation for the stream function ψ

The difference scheme of eq. (2.1c) is discretized by central differences and solved by a line (r direction) SOR iterative method with a value 1.5 of parameter. The test of iteration convergence is as follows:

$$\frac{\max|\psi_{i,j}^{n+1(s+1)} - \psi_{i,j}^{n+1(s)}|}{\max|\psi_{i,j}^{n+1(s+1)}|} \leqslant 10^{-4} \tag{3.13}$$

where s is the iteration number.

4. Criterion of convergence towards a steady state solution

Let

$$R_\phi^n = \frac{\max|\phi_{i,j}^{n+1} - \phi_{i,j}^n|}{\max|\phi_{i,j}^{n+1}|}, \qquad \phi=\zeta,\psi,\theta.$$

The criterion of convergence towards a steady state solution is as follows

$$\frac{1}{\Delta t}\max\{R_\zeta^n, R_\phi^n, R_\theta^n\} \leqslant E_{ps} \tag{3.14}$$

Except for being otherwise stated, the value is $E_{ps}=10^{-3}$.

IV. Results and Discussion

The analysis in 3.2 showed that although there is no limit in ADI method (3.6) on time step Δt, the choice of Δt exerts effects on the truncation error of scheme (3.6) for a steady flow. In order to investigate the effect of choosing Δt on the accuracy of simulation, the numerical results with several time steps under a typical group of parameter values are shown in table 1 and table 2 for a uniform and a nonuniform mesh, respectively. It is not difficult to know by comparing these results that there is no significant effect of time step Δt on the results, except for vorticity ζ . As far as the vorticity is concerned, the effects of time step Δt on the results is also minor for sufficiently small Δt(here$\Delta t \leqslant 0.3$). In tables 1 and 2, the relative errors of all the variables are found less than10%.

The results accounting for the selection of mesh size are listed in tables 3 and 4, from which we conclude that the effects of mesh are conspicuous. For example, the relative error of values of vorticity ζ between mesh 11×11 and mesh 41×41 in table 3 reaches 46.7% . Hence, the sufficiently finer mesh should be used to produce numerical solutions with better accuracy. The relative errors of all the variables between mesh 31×31 and mesh 41×41 in table 3 are less than 7% . Then fairly accurate solutions can be obtained if the uniform mesh 31×31 is employed.

Table 1 Effect of choice of Δt on accuracy of solutions $R_\sigma=10^3$, $M_a=10^3$, $G_r=1$, $\tau=0$, $I\times J=31\times 31$ (uniform mesh), $a=0.5$

Δt	$\max\lvert\psi\rvert$	$\max\lvert u\rvert$	$\max\lvert v\rvert$	$\max\lvert\zeta\rvert$	$\psi\left(\frac{1}{2},\frac{1}{2}\right)$	$\theta\left(0,\frac{1}{2}\right)$	$\theta\left(\frac{1}{2},\frac{1}{2}\right)$	$\theta\left(1,\frac{1}{2}\right)$	CPU time
0.5	3.94(−3)*	2.74(−2)	3.77(−2)	13.16	−1.75(−3)	0.159	0.306	0.669	1111**
0.3	3.96(−3)	2.77(−2)	3.79(−2)	7.80	−1.76(−3)	0.157	0.305	0.668	1556
0.1	4.04(−3)	2.85(−2)	3.82(−2)	8.06	−1.82(−3)	0.168	0.314	0.673	3143
0.03	3.97(−3)	2.85(−2)	3.80(−2)	8.00	−1.76(−3)	0.157	0.304	0.668	8023

*: $a(-b)$ means

**: The unit of CPU time is second, and all the calculations are performed on Micro VAX 2 computer

Table 2 Effect of choice of Δt on accuracy of solutions $R_\sigma=10^3$, $M_a=10^3$, $G_r=1$, $\tau=0$, $I\times J=21\times 21$ (nonuniform mesh, $b=2$), $a=0.5$

Δt	$\max\lvert\psi\rvert$	$\max\lvert u\rvert$	$\max\lvert v\rvert$	$\max\lvert\zeta\rvert$	$\psi\left(\frac{1}{2},\frac{1}{2}\right)$	$\theta\left(0,\frac{1}{2}\right)$	$\theta\left(\frac{1}{2},\frac{1}{2}\right)$	$\theta\left(1,\frac{1}{2}\right)$	CPU time
0.5	3.92(−3)	2.79(−2)	3.79(−2)	14.79	−1.73(−3)	0.159	0.302	0.672	315
0.3	3.94(−3)	2.84(−2)	3.81(−2)	8.77	−1.74(−3)	0.158	0.302	0.671	471
0.1	4.00(−3)	2.92(−2)	3.84(−2)	8.01	−1.79(−3)	0.166	0.308	0.674	1104
0.03	3.95(−3)	2.93(−2)	3.83(−2)	7.95	−1.74(−3)	0.154	0.300	0.669	3239

Table 3 Effect of mesh on accuracy of solutions $R_\sigma=10^3$, $M_a=10^3$, $G_r=1$, $\tau=0$ (uniform mesh), $\Delta t=0.1$, $a=0.5$

$I\times J$	$\max\lvert\psi\rvert$	$\max\lvert u\rvert$	$\max\lvert v\rvert$	$\max\lvert\zeta\rvert$	$\psi\left(\frac{1}{2},\frac{1}{2}\right)$	$\theta\left(0,\frac{1}{2}\right)$	$\theta\left(\frac{1}{2},\frac{1}{2}\right)$	$\theta\left(1,\frac{1}{2}\right)$	CPU time
11×11	3.80(−3)	1.87(−2)	2.11(−2)	4.62	−1.53(−3)	0.116	0.218	0.568	379
21×21	3.90(−3)	2.52(−2)	3.29(−2)	6.88	−1.69(−3)	0.146	0.282	0.650	1368
31×31	4.04(−3)	2.85(−2)	3.82(−2)	8.06	−1.82(−3)	0.168	0.314	0.673	3143
41×41	4.09(−3)	2.98(−2)	4.12(−2)	8.67	−1.86(−3)	0.170	0.322	0.678	6173

Table 4 Effect of mesh on accuracy of solutions $R_\sigma=10^3$, $M_a=10^3$, $G_r=1$, $\tau=0$ (nonuniform meshes ($b=2$), $\Delta t=0.1$, $a=0.5$

$I\times J$	$\max\lvert\psi\rvert$	$\max\lvert u\rvert$	$\max\lvert v\rvert$	$\max\lvert\zeta\rvert$	$\psi\left(\frac{1}{2},\frac{1}{1}\right)$	$\theta\left(0,\frac{1}{2}\right)$	$\theta\left(\frac{1}{2},\frac{1}{2}\right)$	$\theta\left(1,\frac{1}{2}\right)$	CPU time
11×11	3.77(−3)	2.23(−2)	2.72(−2)	5.36	−1.64(−3)	0.114	0.239	0.611	357
21×21	4.00(−3)	2.92(−2)	3.84(−2)	8.01	−1.79(−3)	0.166	0.308	0.674	1104

The comparison of table 3 with table 4 also implies that the more accurate solution can be obtained if a nonuniform mesh (3.2) is preferred to a uniform mesh with the same number of grid points. For example, the results obtained by using the nonuniform mesh 21 × 21 nearly have the same accuracy with those obtained by using the uniform mesh 31 × 31.

The results with different Marangoni number and values of controlling parameter r are illustrated in table 5. Figs. 2a – c, 3a – c and 4a – c describe the configurations of temperature θ, stream function ψ and vorticits ζ with $M_a = 1000$ and several different values of controlling parameter r, respectively. It can be seen from table 5 and Figs. 2 – 4 that the adverse air jet control (i.e. $\tau > 0$) slows down the convection and reduces the variation of temperature θ in radial direction (i.e., it reduces the twist degree of isotherms), and that the favourable air jet control (i.e. $\tau < 0$) speeds up the convection and increases the variation of temperature θ in radial direction, which seems to agree well with the physical arguments. For more detailed analyses in this respect, refer to [6].

Table 5 Effect of control and M_a values on flow $R_\sigma = 10^3$, $M_a = 10^3$, $G_r = 1$, $r = 0$, nonuniform meshes, 21 × 21 (b = 2), $a = 0.5$

M_a	τ	$\max\|\psi\|$	$\max\|u\|$	$\max\|v\|$	$\max\|\zeta\|$	$\psi\left(\frac{1}{2},\frac{1}{2}\right)$	$\theta\left(0,\frac{1}{2}\right)$	$\theta\left(\frac{1}{2},\frac{1}{2}\right)$	$\theta\left(1,\frac{1}{2}\right)$
	0.5	4.34(−3)	2.55(−2)	4.44(−2)	1.46	−1.83(−3)	0.414	0.436	0.562
100	0.0	7.62(−3)	4.93(−2)	7.68(−2)	3.43	−3.10(−3)	0.362	0.387	0.596
	−0.5	1.04(−2)	7.12(−2)	0.104	5.72	−4.19(−3)	0.324	0.347	4.611
	0.5	1.78(−3)	1.81(−2)	2.43(−2)	4.30	−7.42(−4)	0.218	0.288	0.652
1000	0.0	3.94(−3)	2.84(−2)	3.81(−2)	8.77	−1.74(−3)	0.158	0.302	0.671
	−0.5	7.86(−3)	4.06(−2)	7.58(−2)	11.31	−3.37(−3)	0.133	0.337	0.599
	0.5	1.19(−3)	1.51(−2)	1.79(−2)	5.83	−4.81(−4)	0.190	0.277	0.672
2000	0.0	3.12(−3)	2.10(−2)	3.25(−2)	11.19	−1.37(−3)	0.143	0.361	0.657
	−0.5	7.56(−3)	3.77(−2)	7.25(−2)	13.64	−3.29(−3)	0.128	0.403	0.576

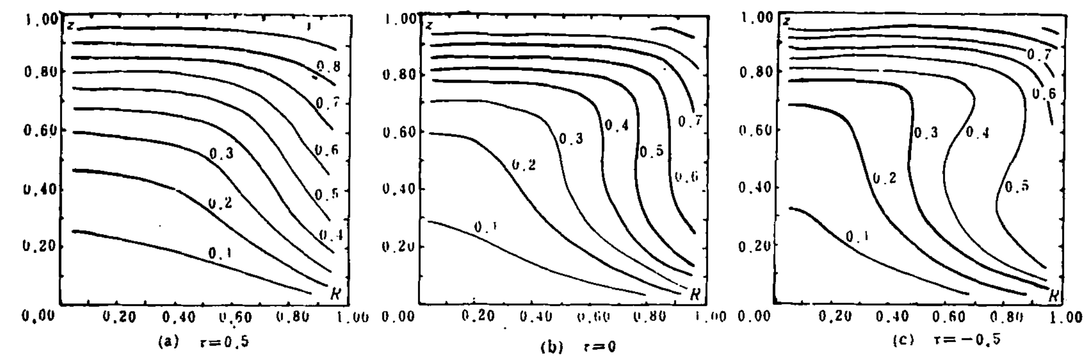

Fig. 2 Isothermals for $R_\sigma = 10^3$, $M_a = 10^3$, $G_r = 1$ and three different control parameters r

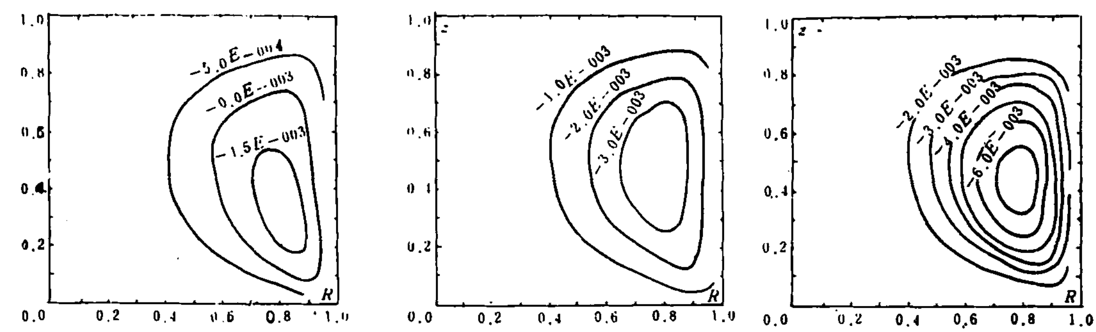

Fig. 3 Flow patterns for $R_\sigma = 10^3$, $M_a = 10^3$, $G_r = 1$ and three different control parameters r

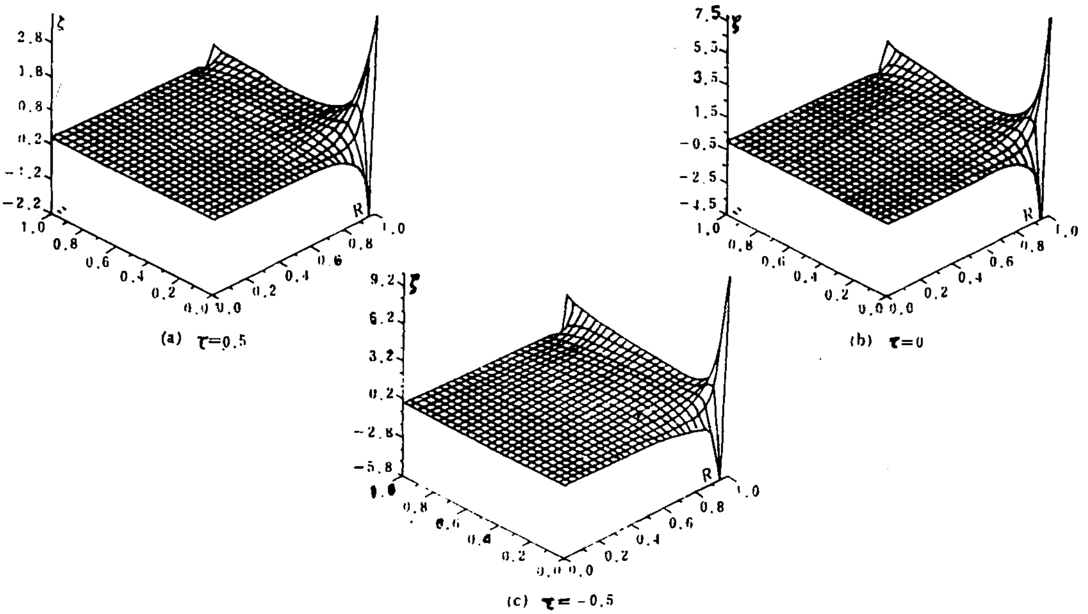

Fig. 4 The configurations of vorticity for $R_\sigma = 10^3$, $M_a = 10^3$, $G_r = 1$ and three control parameters r

The under-relaxation factor α is taken as 0.5 in all the calculations in this paper. The results in Table 1 and Table 2 also indicate that the iterations are convergent for either greater or smaller time steps, implying a feature of scheme (3.6): the requirements on relaxation factor α of the scheme are not severe for medium Reynolds numbers. There are more detailed discussion about this point in [1].

Based on the discussion above we are able to come to the following conclusions:

1° The ADI method proposed by this paper can be used successfully and efficiently to simulate the Marangoni convection control in liquid bridge model. The results turn out both accurate in mathematics and reasonable in physics.

2° Although the spacial truncation error of ADI method (3.6) in involving the effect of time step Δt is not of order 2, the influence of Δt on the accuracy of numerical solutions is minor. One can manage to solve the problems with good accuracy by adopting suitable scheme with nonuniform meshes.

3° It is easier to treat the boundary conditions for intermediate variables by using this kind of scheme. Furthermore, the requirements in choosing (boundary) relaxation factor are not so severe for medium Reynolds numbers.

References

[1] T. Alziary de Roquefort and G. Grillaud, Computation of Taylor vortex flow by a transient implicit method, *Computers and Fluids*, **6** (1978), 259–269.

[2] Kamotani, Y. and J. Kim, Effects of zone rotation on oseillatory thermocapillary flow in a simulated floating zone, *Journal of Crystal Growth*, **87** (1988), 62–68.

[3] Ostrach, S., Low gravity fluid flows, *Ann. Rev. Fluid. Mech.*, **14** (1982), 313–345.

[4] Tang, Z.M. and J.C. Li, *Proceedings of the 4th ACFM*, Hong Kong (1989), *Acta Mechanica Sinica*, **23**, 2 (1991), 149–156.

[5] Huang, W.Z. and S.C. Zhang, Effect of treatment of neumann boundary conditions on accuracy of finite difference solutions, *J. Num. Methods & Com. Appl.*, (to appear) (in Chinese)

[6] Li. J.C., W. Huang., Z.H. Xie and S.C. Zhang, The management of thermocapillary convection in floating zone under microgravity, *Scientia Sinica*. (to appear)